



The Pan-African High-K I-Type Granites From Batié Complex, West Cameroon: Age, Origin, and Tectonic Implications

Maurice Kwékam^{1*}, Victor Talla², Eric Martial Fozing¹, Jules Tcheumenak Kouémo³, István Dunkl⁴ and Eammanuel Njonfang⁵

¹ Laboratoire de Géologie de l'Environnement, Faculté des Sciences, Université de Dschang, Dschang, Cameroon, ² Département Sciences de la Terre, Université de Yaoundé I, Yaoundé, Cameroon, ³ Département Sciences de la Terre, Université de Douala, Douala, Cameroon, ⁴ Department of Sedimentology, Geowissenschaftliches Zentrum Göttingen, Georg-August-Universität Göttingen, Göttingen, Germany, ⁵ Laboratoire de Géologie de l'Ecole Normale Supérieure, Université de Yaoundé I, Yaoundé, Cameroon

OPEN ACCESS

Edited by:

J. Gregory Shellnutt,
National Taiwan Normal University,
Taiwan

Reviewed by:

M. P. Manu Prasanth,
National Taiwan Normal University,
Taiwan
Dominique Gasquet,
Université Savoie Mont Blanc, France

*Correspondence:

Maurice Kwékam
maurice.kwekam@univ-dschang.org;
mkwekam@yahoo.fr

Specialty section:

This article was submitted to
Petrology,
a section of the journal
Frontiers in Earth Science

Received: 16 April 2020

Accepted: 04 August 2020

Published: 09 September 2020

Citation:

Kwékam M, Talla V, Fozing EM, Tcheumenak Kouémo J, Dunkl I and Njonfang E (2020) The Pan-African High-K I-Type Granites From Batié Complex, West Cameroon: Age, Origin, and Tectonic Implications. *Front. Earth Sci.* 8:363. doi: 10.3389/feart.2020.00363

The Batié granitic massif in western Cameroon is NE–SW elongated, follows the regional foliation, and is parallel to the Kekem–Fotouni shear zone, which is the southwestern extension of the Tcholliré–Banyo Fault (TBF). This massif comprises two petrographic units: biotite granite and amphibole granite. Major, trace, REE, Sr–Nd isotopic, and new U–Pb data are used to constrain their nature and origin. The results indicate that they are high-K alkali-calcic with shoshonite affinity. The amphibole granite is metaluminous, whereas biotite granite is weakly peraluminous. Both granites are high-temperature I-type granites and crystallized under oxidizing conditions. Initial (⁸⁷Sr/⁸⁶Sr)_{620 Ma} ratios (0.7062–0.7080) and εNd_{620 Ma} (–12.6 to –8.9) indicate that the parental magmas were produced by partial melting of thick Paleoproterozoic crust and were mixed with felsic magma from the upper continental crust. Their Nd T_{DM} typically varies from 1.68 to 1.96 Ga. The massif was mostly emplaced between 630 and 547 Ma during the transitional period between the crustal thickening (630–610 Ma) and the development of the shear zones, which began with sinistral movements (610–580 Ma) and continued with dextral movements (585–540 Ma). Plutonism continued during the dextral movements. The Batié granite is geochemically and isotopically similar to other post-collisional pan-African granitic massifs located along the TBF.

Keywords: Batié massif, Pan-African, Paleoproterozoic crust, collision, high-K granite

INTRODUCTION

The Pan-African domain of Western Central Cameroon shows many plutonic massifs emplaced following the extensive remobilization and granitization during the collision between the São Francisco–Congo and West African cratons and the Saharan metacraton at 640–580 Ma (Liégeois et al., 1998; Abdelsalam et al., 2002; Ngako et al., 2008). The Pan-African geological history of this domain indicates that there have been several magmatic episodes of rock formation from various sources (crustal or mantle) in different tectonic settings (pre- to post-collision). Plutonic rocks were emplaced into shear zones and are either foliated or unfoliated. Deformation usually occurred either

during or immediately after the consolidation of the magma. The elongated NE–SW Batié plutonic massif outcrops at the southern edge of the Kekem–Fotouni shear zone, which is the southwestern extension of the Tcholliré–Banyo Fault (TBF). Along this shear zone and on either side, several granitic massifs were studied. They are mainly I- or S-type, which are high-K calc-alkaline granites emplaced between 680 and 580 Ma (Nzolang et al., 2003; Tagne-Kamga, 2003; Toteu et al., 2004; Tchameni et al., 2006; Djouka-Fonkwé et al., 2008; Kwékam et al., 2010, 2013, 2020).

In this study, we focus on the Batié magmatic complex, along with a large number of similar Pan-African granitoids, emplaced along the TBF that separates the Central from the Northern domain. The field associations, combined with geochemical, zircon U–Pb, and whole-rock Sr–Nd isotopic studies, provide important constraints on the source nature and mechanism for the formation of this pluton, which in turn might have great significance in understanding the Neoproterozoic Pan-African belt in West Cameroon. Our results show that the partial melting of materials of mixed origin at the continental crust during the Pan-African orogeny would be a plausible process in the formation of Batié granite.

GEOLOGICAL SETTING

The convergence between the São Francisco–Congo and West African craton and the Saharan metacraton during the late Neoproterozoic gave rise to the Pan-African Central African Fold Belt (CAFB) (Abdelsalam et al., 2002). The edges of the cratons were brittle and remobilized by the various metamorphic episodes and deep faults that segmented the continental lithosphere into blocks delineated by post- to late-collisional shear zones. Liégeois et al. (2013) distinguish metacratonized and non-metacratonized domains (**Figure 1**).

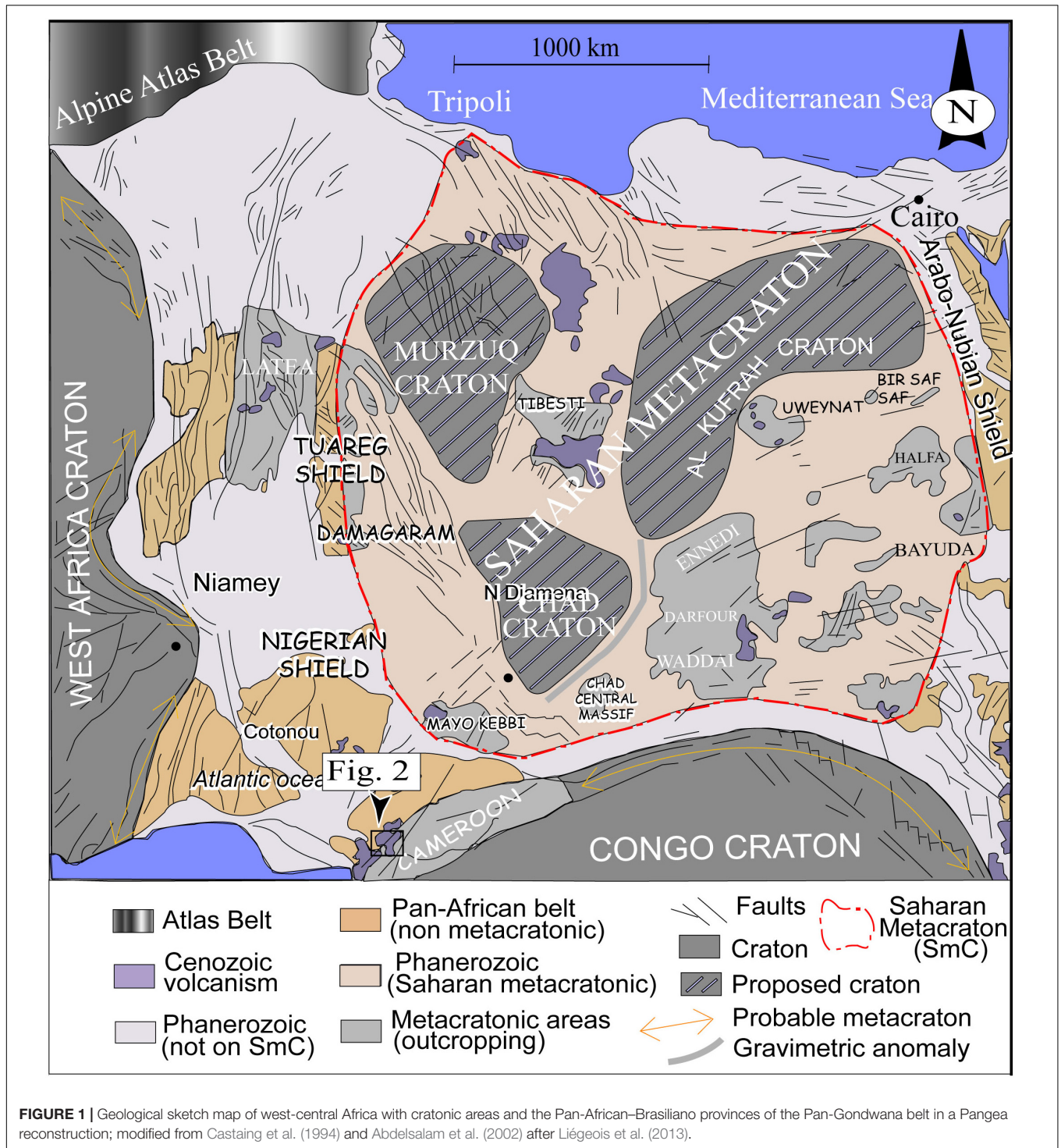
Three main successive tectonic events, associated with the Pan-African collisional and post-collisional evolution, are defined in Cameroon (Ngako et al., 2008): (i) crustal thickening (630–610 Ma) marked by refolded thrust tectonics and widespread stretching lineation, (ii) left lateral wrench movements (610–580 Ma), and (iii) right lateral wrench movements mainly presented in the Central Cameroon shear zone (CCSZ) and dated at 585–540 Ma (Toteu et al., 2004). This evolution ends with the development of the molassic basins and the emplacement of alkaline granitoids at 545 Ma in the context of distension (Toteu et al., 2004; Dawai et al., 2013; Bouyo-Houketchang et al., 2016). Many regional syntheses distinguish three tectonic domains in the CAFB: West Cameroon, Central Cameroon, and South Cameroon. The West Cameroon domain, defined as an active margin, is characterized by a calc-alkaline magmatism from 800 to 600 Ma (Toteu et al., 2001). It is marked by elongated granitic massifs aligned in the NE–SW direction parallel to the regional schistosity (Tetsopgang et al., 2008; Fozing et al., 2014; Njanko et al., 2017; Kwékam et al., 2020). The Central Cameroon domain is an intermediate continental domain and consists of Pan-African granitoids intruding gneissic basement. This domain

is also highlighted by many shear zones along which outcrops granitic massifs with associated amphibolite enclaves (Fozing et al., 2019). Granitic massifs are generally elongated parallel to the NE–SW shear zones and are emplaced in transpression or transtension fault relay zones (pull-apart basins). This is the case of the Lom granite (Ngako et al., 2003), the Bandja granite (Nguessi-Tchankam et al., 1997; Tcheumenak Kouémo et al., 2014), and the Bangangté syenite (Tchouankoué et al., 2016). Most of these massifs are calc-alkaline and strongly potassic, which are I- or S-type with shoshonitic affinity (Nzolang et al., 2003; Djouka-Fonkwé et al., 2008). The central domain is separated from the western domain by the TBF. The southern domain represents a syntectonic basin (Toteu et al., 2006). It includes meta-sediments and pre- to syntectonic intrusions metamorphosed in the granulite facies (Nzenti et al., 1992) before exhumation and thrusting over the Congo craton (Barbey et al., 1990).

The Kekem–Fotouni shear zone, which separates the Fomopéa granite from the Bandja and Batié massifs, is marked by a mylonite band affecting Paleoproterozoic gneisses (ca. 2.1 Ga; Penaye et al., 1993) and the edges of the granitic massifs. In this mylonite band, small plutons of gabbro-norite (Kwékam et al., 2013) and charnockite are also observed (Nguessi-Tchankam et al., 1997; Tcheumenak Kouémo et al., 2014). These formations, as well as the granites from the remobilized gneisses, are largely covered by the Tertiary transitional basalt of Mount Bangou and the Cenozoic volcanic rocks of Mount Bambouto (**Figure 2A**).

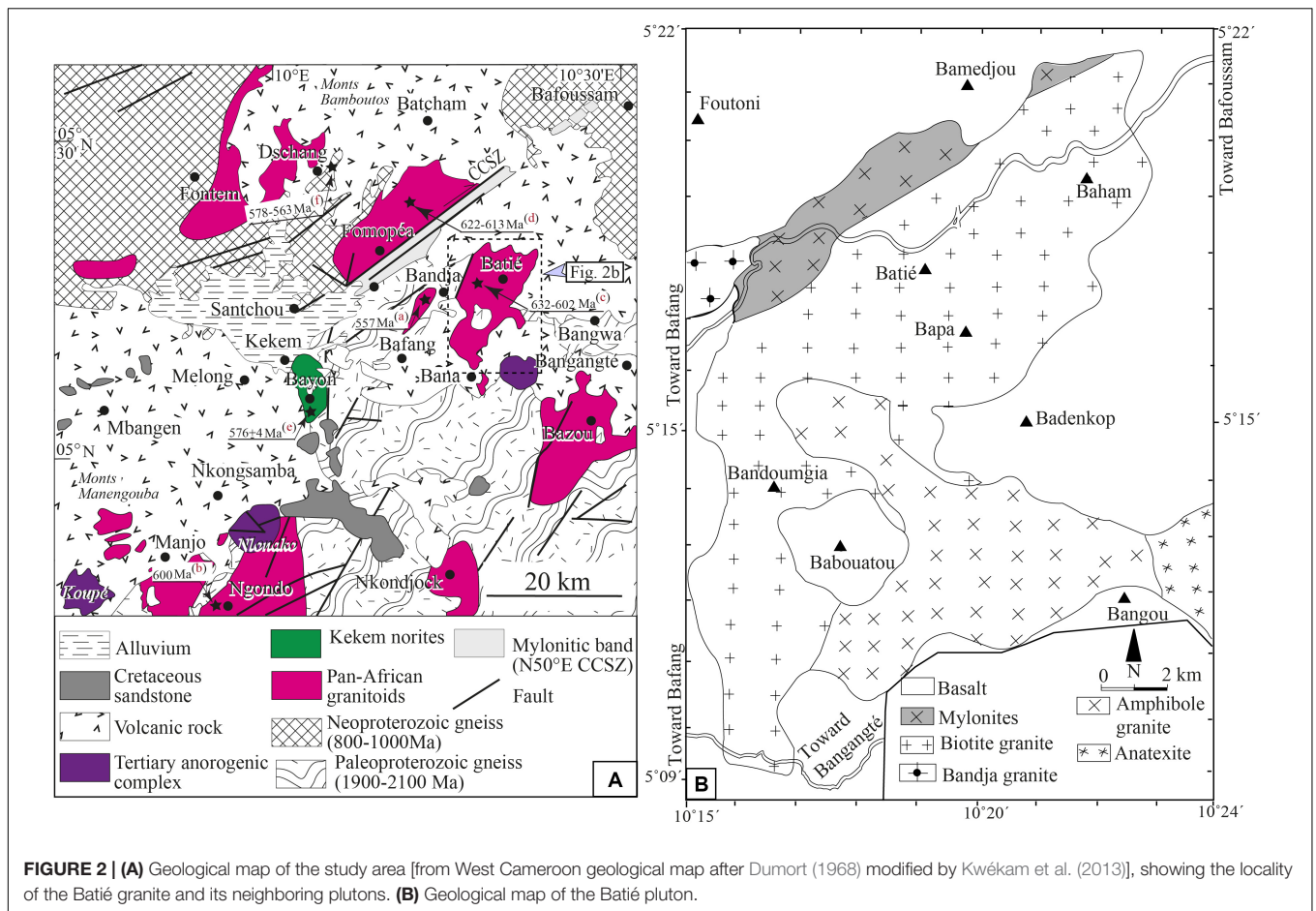
FIELD GEOLOGY AND PETROGRAPHY

The Batié granitic complex is elongated NE–SW and parallel to the other granitic massifs that outcrop along the Kekem–Fotouni shear zone (**Figure 2A**). This syn-kinematic characteristic is underlined within the massif by NNE–SSW elongated micro-enclaves parallel to the preferential orientation of the feldspar megacrystals and granitic dykes (pegmatite) with oblique internal prismation, suggesting a sinistral NNE–SSW syn-magmatic shear. The Batié granite massif intrudes an orthogneiss complex, but the contact is entirely concealed by Tertiary volcanic formations of Mount Bangou (**Figure 2B**). Its northwestern edge is affected by the Kekem–Fotouni shear zone. Petrographically, it primarily consists of biotite granite and amphibole granite. The amphibole granite is exposed to the southeast and northwest of the massif. The Batié granite is leucocratic with an oriented porphyritic structure, which is characterized by the abundance of K-feldspar megacrystals that range in size from 5 to 8 cm length and from 2.5 to 5 cm width. These crystals show mostly symmetrical Carlsbad's twin and preferentially NNE–SSW orientation. In addition to K-feldspar, this granite consists of quartz, plagioclase, biotite, and/or amphibole. Titanite, allanite, apatite, zircon, and magnetite are identified as accessory minerals. Quartz (24–40%) is interstitial and occurs in polycrystalline clusters frequently wedged between the feldspar megacrystals. K-feldspar (15–38%) is orthoclase, which is sometimes transformed into microcline at the edge or entirely. It is euhedral to sub-euhedral and develops exsolutions



of plagioclase (lamellae and staining perthite). It encloses titanite, biotite, apatite, and magnetite crystals. It is replaced by sericite. Plagioclase (22–31%) occurs as euhedral to sub-euhedral crystals (2 cm × 1 cm), which is classified as oligoclase (An_{26–17}). It often displays albite and Carlsbad’s twin and has normal zoning. Alteration is frequent, especially from the core. Plagioclase in the amphibole granite (northwestern edge) displays mechanical

twinning and kink-band deformation. Biotite (2–13%) occurs as flakes with frayed ends and corroded by quartz and feldspars. The biotite flakes form isolated crystals and discontinuous lines surrounding the feldspar megacrystals. Biotite also contains apatite, titanite, zircon, magnetite, and allanite. Some flakes are altered to chlorite. Amphibole (0.7–4%) is a green hornblende found only in the amphibole granite. It occurs in euhedral to



sub-euhedral cross-sections with frequent h1 (100) twinning and generally sub-euhedral longitudinal sections.

Secondary, epidote, chlorite, and sericite are present in minor abundances.

ANALYTICAL METHODS

Mineral Analyses

The chemical composition of amphiboles, biotite, and feldspar is determined on 10 thin polished slides using the Cameca SX50 automated electron microprobe at the Institute of Mineralogy and Petrography of the Swiss Federal Institute of Technology in Zurich. Natural and synthetic silicates were used as calibration standards, and the raw data are automatically corrected for deviation, dead time, and background noise using the ZAF correction process (Pouchou and Pichoir, 1984). The conditions of analysis are set at 15 kV and 20 nA with 200 s counting time for one element.

Laser Ablation U-Th-Pb Analyses

Sample BT901 of the amphibole granite collected for U-Th-Pb geochronology by laser ablation was crushed, and the zircon crystals were separated by the heavy liquid and magnetic

separation method using conventional techniques (e.g., Bosch et al., 1996). The non-magnetic zircon crystals were hand sorted and mounted on double-sided adhesive tape and embedded in a 25 mm diameter epoxy support. The crystal supports were coated with 2,500 mesh SiC paper and polished with 9, 3, and 1 μm diamond suspensions.

The analytical method is described in detail by Kwékam et al. (2020). The age calculation and quality control are based on the drift and fractionation corrections by standard-sample bracketing using GJ-1 zircon reference material (Jackson et al., 2004). Deviations, splitting corrections, and data reductions were performed using the Geozentrum Göttingen, Georg-August Universität, Abteilung Geochemie's UranOS software (Dunkl et al., 2008). The quality and accuracy of the method was verified by analyses of secondary reference materials: the Plešovice zircon yielded a concordia age of 337.1 ± 1.0 Ma (Sláma et al., 2008) and the 91500 zircon yielded a concordia age of $1,059.6 \pm 3.8$ Ma (reference age of $1,065.4 \pm 0.3$ Ma; Wiedenbeck et al., 1995). The concordia curve was obtained using the Isoplot software (Ludwig, 2012).

Whole-Rock Geochemical Analyses

The whole-rock geochemical analysis was performed by X-ray fluorescence (XRF) and inductively coupled plasma mass

spectrometry (ICP-MS) at the Institute for Mineralogy and Petrography (IMP) of the Swiss Federal Institute of Technology Zurich (ETH Zurich) and at the Geozentrum Göttingen, Georg-August Universität, Abteilung Geochemie, Germany. Major and some trace elements (Sc, V, Cr, Co, Ni, Zn, Ga, Rb, Sr, Zr, and Ba) are measured by XRF analysis on glass disks (see detail in Kwékam et al., 2020).

Rb–Sr and Sm–Nd Isotopic Analyses

Hundred milligram of the samples was dissolved by an acid mixture of HNO₃ and HF at 180°C. The separation of Sr and REE was performed on columns filled with the cation exchange resin AG 50W-X8 with 2.5 M HCl. Nd separation from the REE was performed on a column filled with hexyl di-ethyl hydrogen phosphate (HDEHP) coated Teflon with 0.18 M HCl. Sr, Nd, Rb, and Sm isotopes were measured with a Finnigan TRITON mass spectrometer at the Geowissenschaftliches Zentrum Göttingen, Georg-August Universität, Abteilung Geochemie. Measurements were performed in static and in the peak-jumping multicollector mode for Sr and for Nd, respectively. Sr analyses were corrected for mass fractionation by normalization to $^{88}\text{Sr}/^{86}\text{Sr} = 8.375209$, whereas Nd analyses were normalized to $^{146}\text{Nd}/^{144}\text{Nd} = 0.7219$. Repeated measurements of the standard NBS987 gave on average a value of 0.710244, with a reproducibility of 0.000007 (2 σ). The Nd standard La Jolla was determined with an average of 0.511845 ± 0.000005 (see detail in Kwékam et al., 2020).

RESULTS

Zircon U–Pb Dating

BT901 From AG

Twenty-one zircons extracted from the BT901 amphibole granite sample have been treated, and data are reported in **Supplementary Table S1**. Zircon crystals are usually in an elongated pyramidal shape. The zircons are translucent and light pink. Th/U is >0.1 and ranges from 0.2 to 1.6, which is the feature of magmatic zircon. The U–Pb ages obtained on the individual grains are Neoproterozoic (683–547 Ma), and we can distinguish two families of zircons. The first is made up of old zircons obtained from two grains (682 and 634 Ma), and the second major group has ages ranging from 612 to 547 Ma. On the concordia diagram, data are scattered and do not permit a reliable age to be determined (**Figure 3A**). However, the “Zircon Age Extractor” method by Ludwig (2012) gives an average age of $561 \pm 8/-5$ Ma with 97.9% confidence coefficient by a coherent group of 10 points (**Figure 3B**). This age is comparable to the Neoproterozoic ages obtained on the neighboring granitic massifs of the central domain of the Pan-African orogeny from Central Africa in Cameroon (Li et al., 2017; Kwékam et al., 2020).

Sample From BG

U–Pb ages on zircons from the biotite granite have already been determined by Njiekak et al. (2008) in an extensive study of the Bangwa and Foubot areas. The old inherited (634–628 Ma) and Neoproterozoic (602–503 Ma) ages were presented

on 10 zircon crystals. The authors had interpreted these data as contamination by the gneissic host rocks for the former (634–628 Ma) and emplacement age (602 Ma) and deformation (mylonitization) age after emplacement of the Batié massif (575 Ma from Talla, 1995). Thus, data obtained for both granites (AG and BG) seem to reflect the geological history of the region, especially the CAFB. Considering the results and the ages of similar massifs in the same region (e.g., Fomopéa granites; 621–613 Ma; Kwékam et al., 2010), we propose the age of intrusion at ~ 630 to ~ 602 Ma.

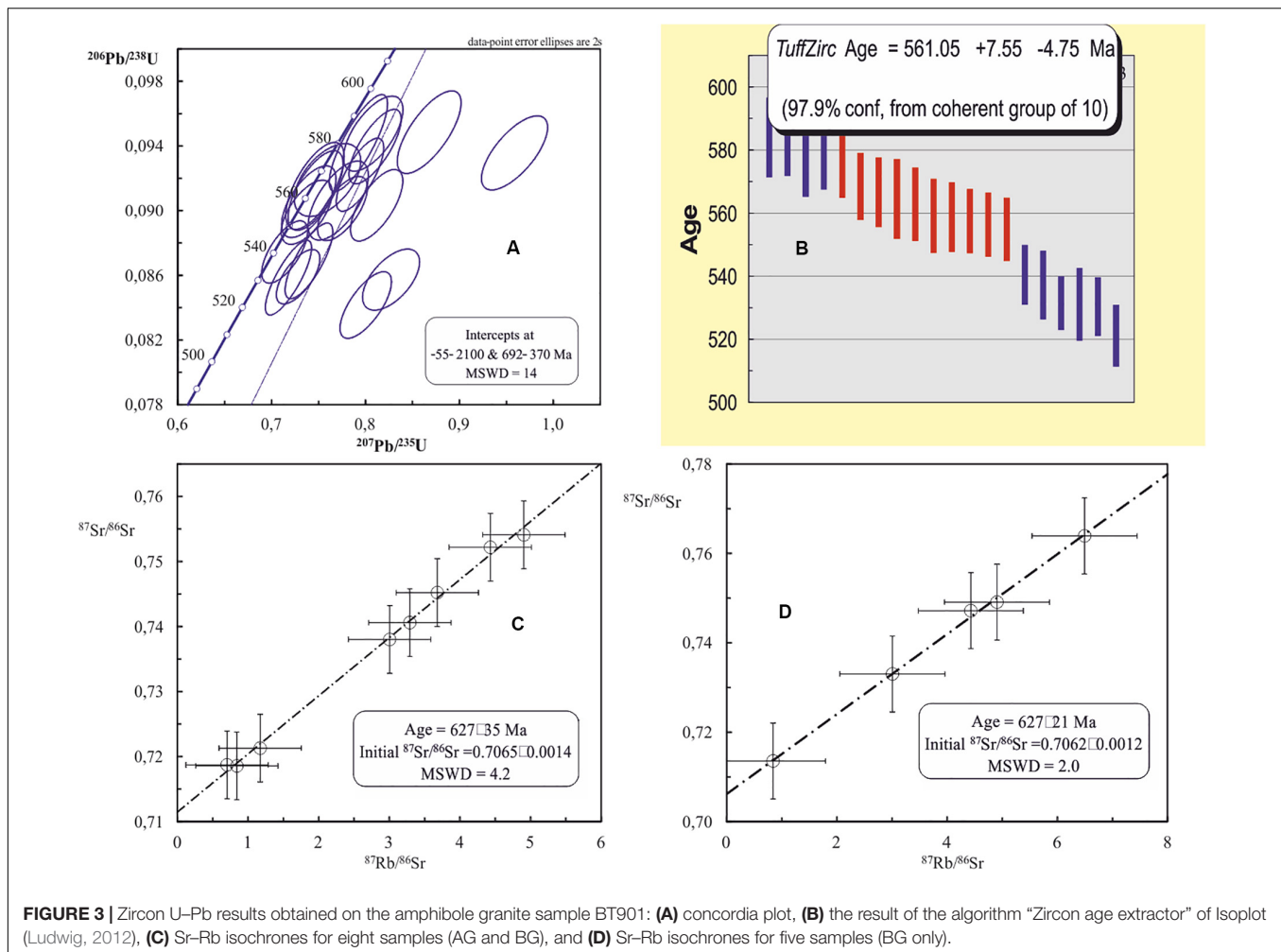
Whole-Rock Sr–Nd Isotopic Compositions

Eleven Sr isotope analyses were performed (**Supplementary Table S2**). Five BG samples and three AG samples define an isochron at 627 ± 35 Ma with $^{87}\text{Sr}/^{86}\text{Sr}$ initial ratio = 0.7065 ± 0.0014 and mean squares of weighted deviates (MSWD = 4.2). Another isochron obtained by five samples of BG indicates 627 ± 21 Ma with $^{87}\text{Sr}/^{86}\text{Sr}$ initial ratio = 0.7062 ± 0.0012 and a really good MSWD = 2.0. The isochron ages have significant uncertainty (**Figures 3C,D**) but cover the range from the zircon U–Pb ages, as well as the ages of the other massifs of the CAFB domain. Initial ($^{87}\text{Sr}/^{86}\text{Sr}$)_{620 Ma} ratios (0.7019–0.7080) of analyzed samples are low and vary only slightly.

Nd isotope data were obtained from four biotite granite samples and one amphibole granite sample (**Supplementary Table S2**). The $\epsilon\text{Nd}_{620 \text{ Ma}}$ (–8.9 to –12.6) isotope parameters and the older model age T_{DM} (1,685–1,963 Ma) suggest a crustal component in the source.

Geochemical Compositions

The SiO₂ contents range from 53 to 68 wt.% in the AG and from 56.3 to 76 wt.% in the BG (**Supplementary Table S1**). Both granites have high K₂O contents of 4.1–8.1 wt.%. In the SiO₂ vs. K₂O diagram (**Figure 4A**), these granites plot mostly within high-K calc-alkaline to shoshonite series fields. K₂O contents decrease in BG with increasing SiO₂. They also classify as alkalic and alkalic granites (**Figure 4B**; Frost et al., 2001). AG are mostly metaluminous (A/CNK = 0.78–1.02), whereas BG are metaluminous to weakly peraluminous (A/CNK = 0.95–1.10); therefore, these are typical I-type granitoids (**Figure 4C**; Chappell and White, 1992). The FeO* (0.72–1) indicates that the rocks of the Batié massif belong to the ferroan series (**Figure 4D**; Frost et al., 2001). MgO, CaO, Al₂O₃, Fe₂O₃, P₂O₅, and TiO₂ contents decrease with increasing SiO₂ (**Figure 5**). However, no significant correlations were noticed in the Na₂O vs. SiO₂ diagram (**Figure 5**). Normalized REE patterns of all samples are generally parallel to each other and to the crust (**Figure 6**). The LREE exhibit moderate to strong enrichment [(La/Yb)_N = 19–68] relative to the primitive mantle, whereas the HREE patterns are almost flat [(Dy/Yb)_N = 1.2–2.2]. BG have strong negative europium anomalies (Eu/Eu* = 0.53–0.14), whereas AG have weak europium anomalies (Eu/Eu* = 0.71). Primitive mantle-normalized trace element diagram shows Th, U, K, and Zr enrichment and Ba, Nb, Sr, P, and Ti depletion (**Figure 6**).



Mineralogy

The amphiboles of the GA of the Batié massif give distinct chemical compositions (**Supplementary Table S3**). The values for Ca (1.67–1.96 a.p.f.u.) and Na (0.04–0.13 a.p.f.u.) in the B-site and their $(Ca + Na)_B$ indicate that these amphiboles belong to the calcium amphibole sub-group after Leake et al. (1997). In addition, the values of Si^{IV} (6.27–7.23) in site T and the sums of $(Na + K)_A$ in site A (0.21–0.66), as well as their $Mg/(Mg + Fe)$ ratios of 0.44–0.79, indicate that the amphiboles of the AG of the Batié massif are magnesio-hornblende, magnesio-hastingsite hornblende, and edenite hornblende in accordance with the classification by Leake et al. (1997). Some crystals of the deformed AG have actinolite and hornblende affinities (**Supplementary Table S3**).

Biotites are present in both granites (AG and BG) and have fairly distinct chemical compositions (**Supplementary Table S4**). The biotites in AG are more magnesian ($MgO = 9.84$ – 15.12%) and depleted in Al_2O_3 (13.75–14.88%) and FeO (15.35–21.79%), whereas the biotites in BG are richer in Al_2O_3 (15.96–16.63%) and FeO (22.40–25.07%) and poor in MgO (5.82–7.55%). Their $Mg/(Mg + Fe^{2+} + Mn^{2+})$ ratios make it possible to distinguish between the two groups of biotites (0.45–0.66 for AG and

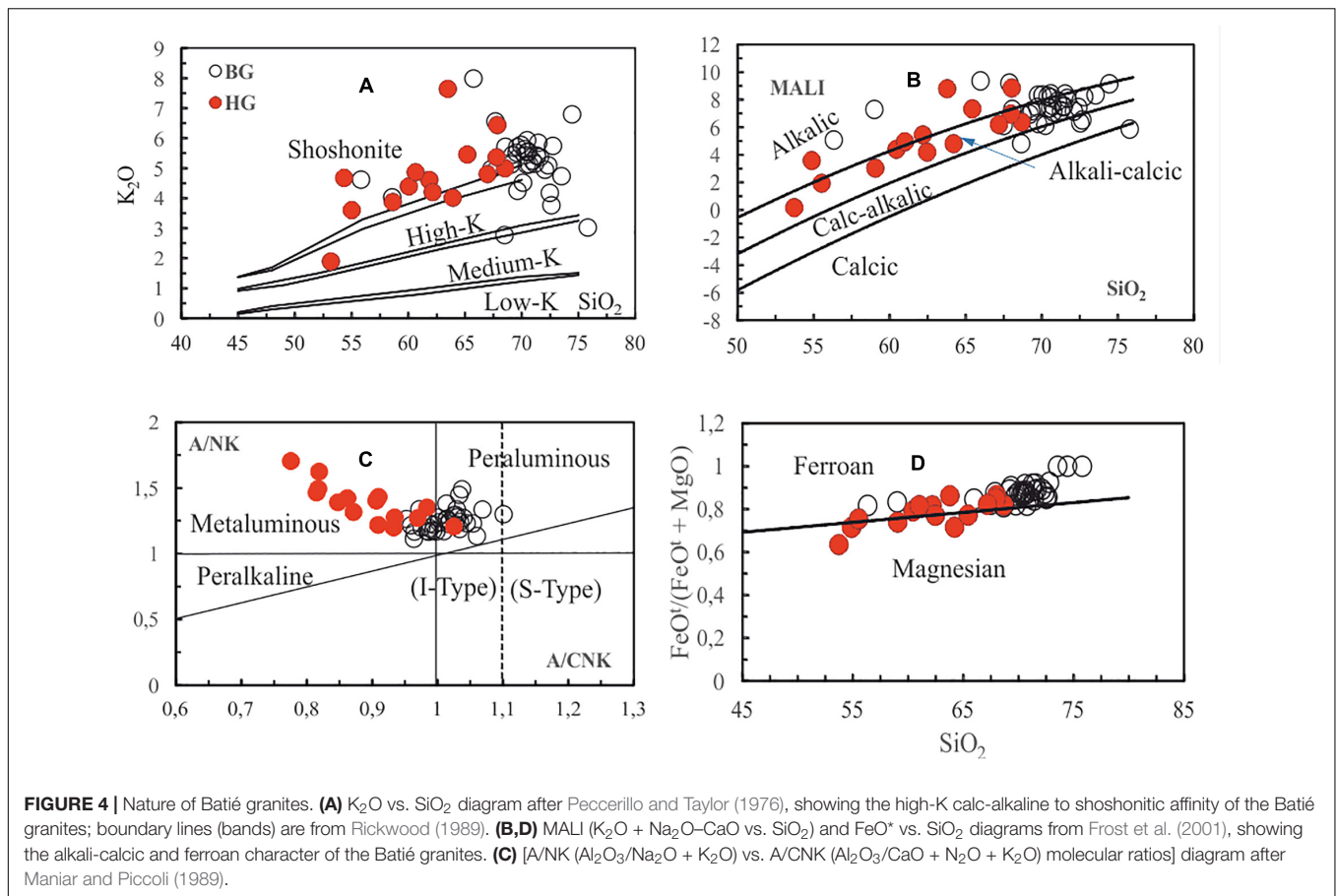
0.29–0.36 for BG). Therefore, the biotites in BG are plotted at the Fe-biotite pole, whereas the biotites in AG extend from the transitional zone between Fe-biotite and Mg-biotite to the Mg-biotite pole in triangular diagram (**Figure 7A**) after Foster (1960). These characteristics of the biotites from the Batié massif are similar to those of the biotites of the metaluminous calc-alkaline granitoids (**Figures 7B,C**; Abdel-Rahman, 1994).

The composition of feldspar varies from labradorite An_{58} to oligoclase An_{13} . Plagioclases are generally oligoclase (An_{26-23}) in the AG; however, zoned crystals show a core of labradorite–andesine (An_{58-48}) composition. The plagioclases in the deformed AG are predominantly albite–oligoclase (An_{23-5}). In the BG, the plagioclases are usually of oligoclase (An_{27-17}) composition.

DISCUSSION

Age

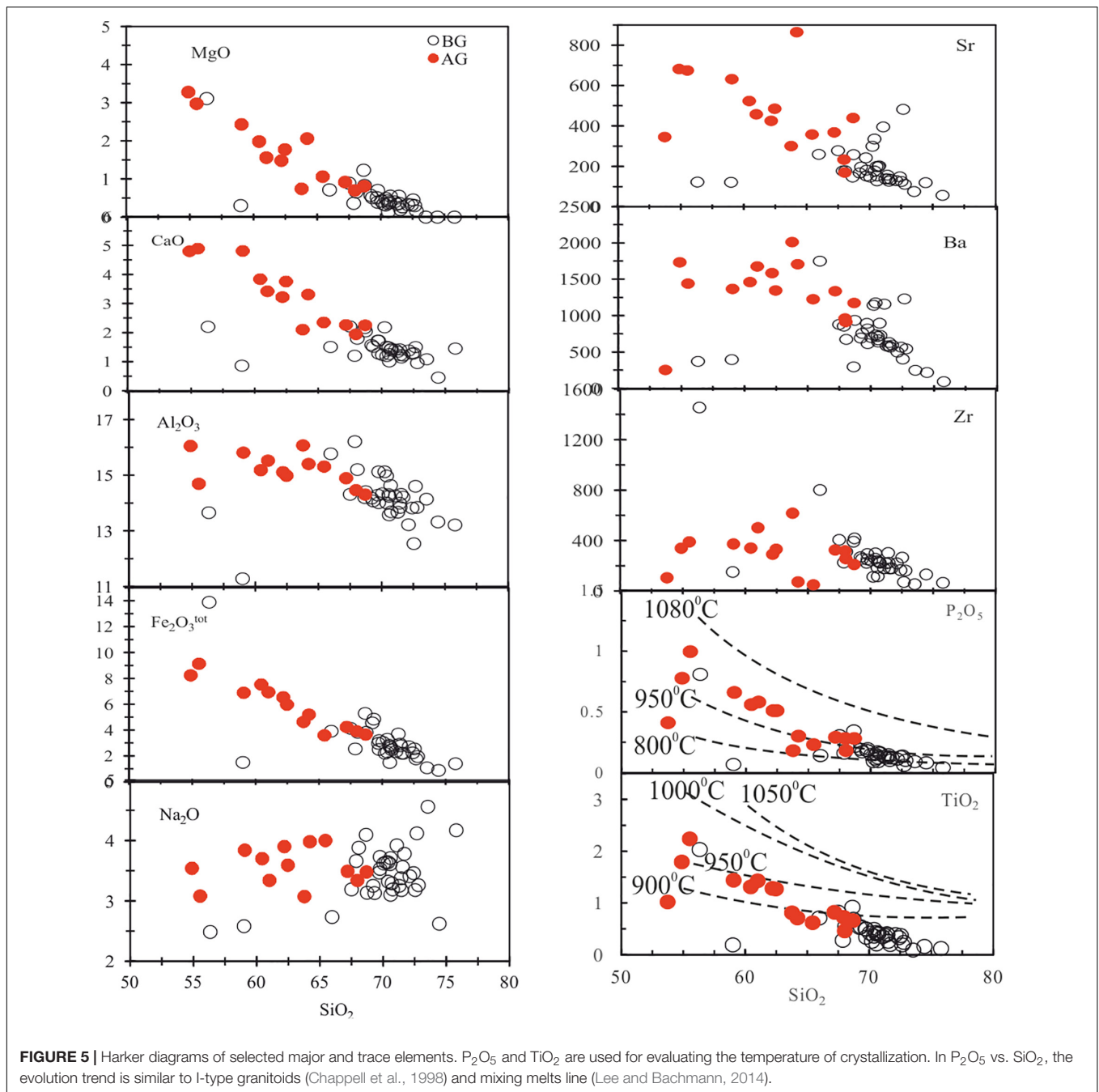
Data obtained for the Batié granite massif is used to reveal the geological history of the CCSZ. The geochronological data (634–503 Ma) by Njiekak et al. (2008) and this work (683–547 Ma)



indicate that the emplacement of the massif lasted at least 100 Ma. The oldest ages (683–634 Ma) can be considered as those of inherited zircons. Wherever a silicic magma is saturated in water, zircon crystallization begins early in the magmatic period and continues up to the end with the development of trace elements rich in hydrozircon (Pupin, 1980). The large size of the feldspar crystals, as well as the mineralogical assemblage of the Batié granites, indicates that the magma was very rich in water. This explains the age range of the zircons of these granites. Considering the Rb/Sr data (627 ± 21 Ma) and the ages obtained in the neighboring massifs (630–572 Ma for Fomopéa, 590–550 Ma for Bandja), the age of the Batié massif can be constrained between 630 Ma and 547 Ma. U–Pb zircon results suggest that the emplacement of the Batié granite began at the end of crustal thickening and, together with the Fomopéa complex, represents the first generation of high-K Pan-African calc-alkaline plutons from western Cameroon. They are thus older than most of the Pan-African plutons that are being emplaced at ca. 580 Ma during the second tectonic period (Kwékam et al., 2010). The age interval likely identifies distinctly the deformation phases that the massif experienced. Indeed, the BT901 sample of amphibole granite was collected in the mylonite band in the NW of the massif, and the ages between 561 and 547 Ma may correspond to the mylonitization phase as suggested by Nguessi-Tchankam et al. (1997), Njiekak et al. (2008), and Kwékam et al. (2013).

Magma Evolution Conditions

The mineralogical composition of the granites, as well as the chemical composition of their ferromagnesian minerals, is generally a function of the evolution conditions of the magma (e.g., degree of oxidation and water content) (Wones, 1981; Bonin, 1990; Ridolfi et al., 2010; Chen et al., 2016). The grain size of the rock is also influenced by the evolution conditions of the magmas (Marre, 1982). The large size of feldspars in the Batié granite, some of which reach more than 5 cm, and the presence of titanite, magnetite, and allanite suggest an oxidizing and H_2O -rich environment. The coexistence of titanite and quartz also suggests high oxygen fugacity (Wones, 1989). For instance (Figure 8), amphibole crystallized from oxidizing magmas would possess higher $Fe^{3+}/(Fe^{3+} + Fe^{2+})$ and lower $Fe/(Fe + Mg)$ ratios than those from the reducing ones (Wones, 1981). The amphiboles from AG are characterized by high $Fe^{3+}/(Fe^{3+} + Fe^{2+})$ ratios of 0.18–0.41 and relatively low to moderate $Fe/(Fe + Mg)$ ratios of 0.44–0.60 and 0.61–0.79, suggesting crystallization under an oxidizing condition (Wones, 1981; Clowe et al., 1988; Chen et al., 2016). On the other hand, total rock K/Rb ratios are relatively low in the biotite granite (49–315) and moderate in the amphibole granite (140–311), indicating a highly evolved magma for the biotite granite to moderately evolved magma for the amphibole granite (Figure 8).

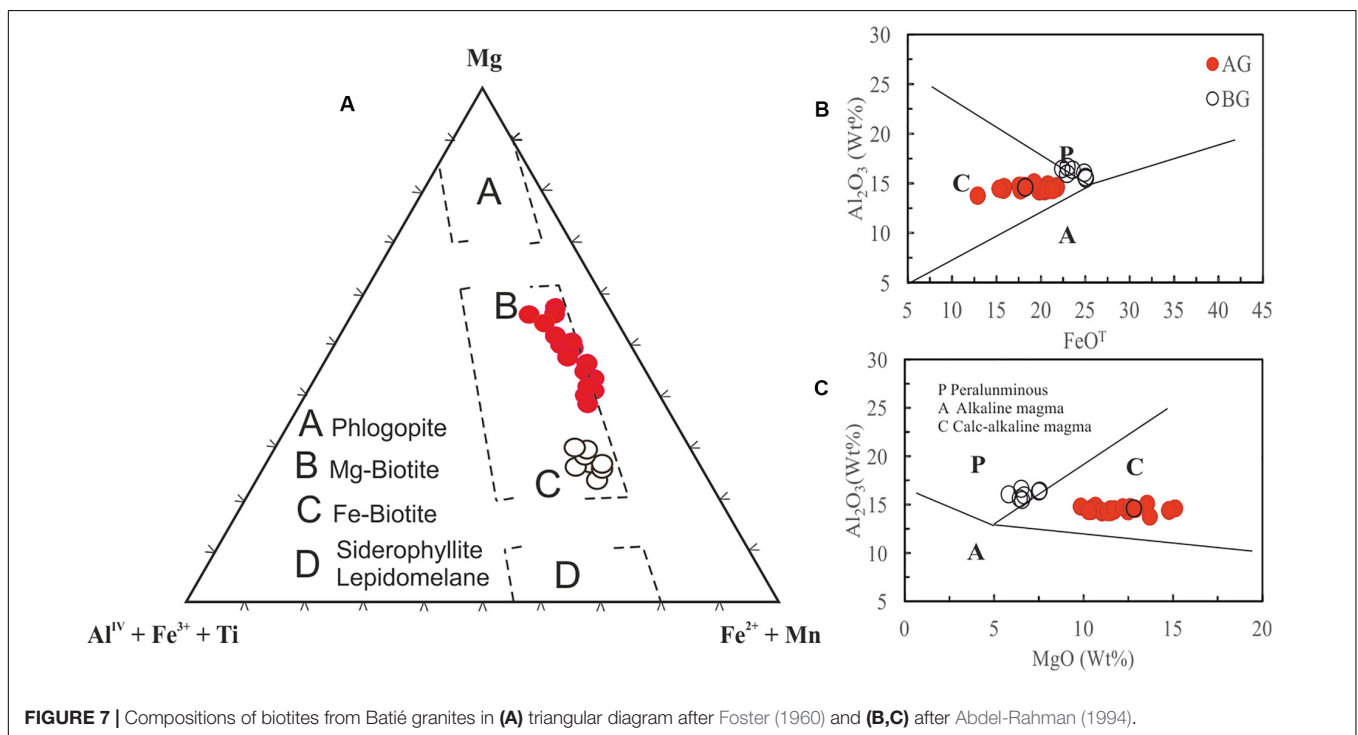
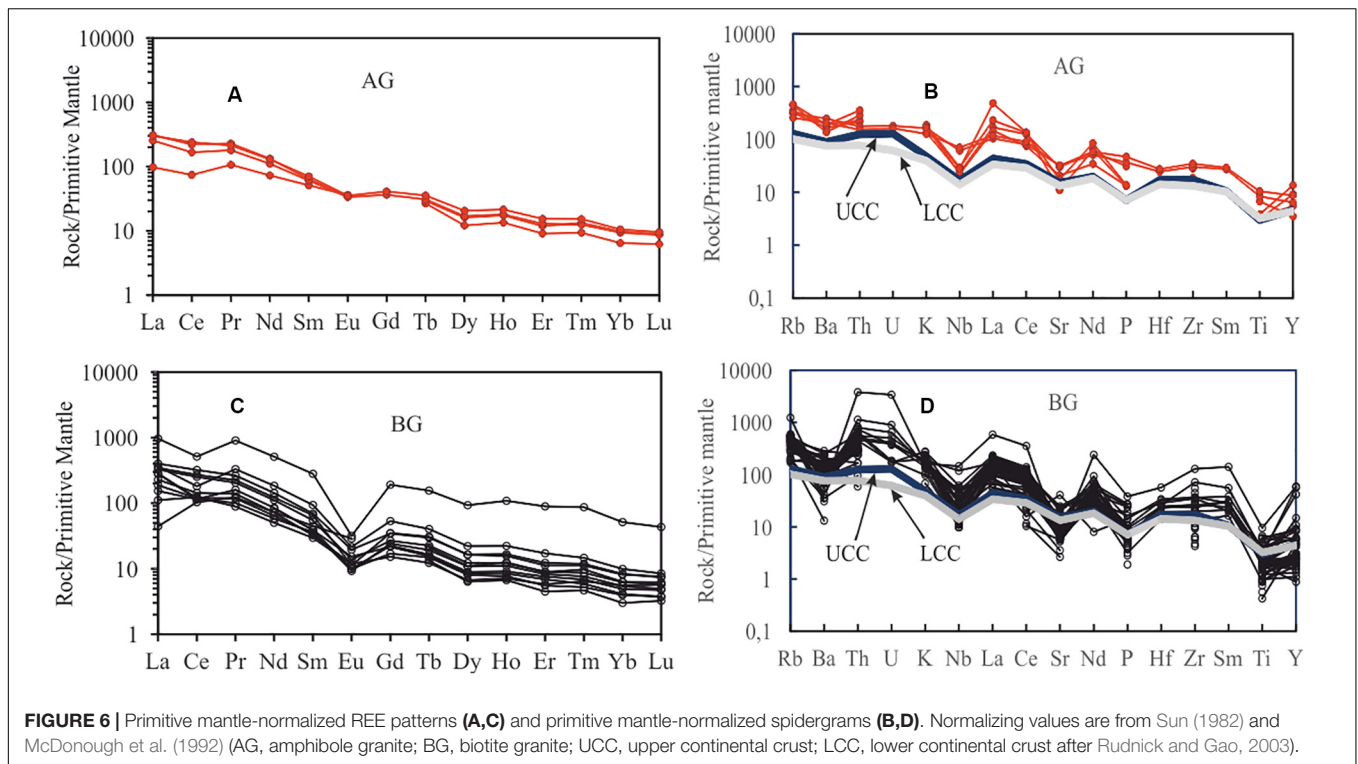


Various authors have shown that there is a linear relationship between the total aluminum of the hornblende and its crystallization pressure (Hollister et al., 1987; Johnson and Rutherford, 1989). The pressures of the AG amphiboles were calculated using the equations proposed by Schmidt (1992), whereas the temperatures were calculated using the thermometry by Blundy and Holland (1990). The AG yielded crystallization temperatures and pressures ranging from 682 to 822°C and from 1.12 to 6.8 kbar, respectively. The temperatures and pressures calculated on the amphiboles are much more representative of the final emplacement conditions. Temperatures obtained

using whole-rock P_2O_5 and TiO_2 contents indicate values well above 950°C (Figure 5). These values, which are related to those of apatite and titanite minerals, suggest that the magma of the granites of the Batié massif started to crystallize at temperatures above 950°C and indicate that these granites are high-temperature I-type granites (Chappell et al., 1998).

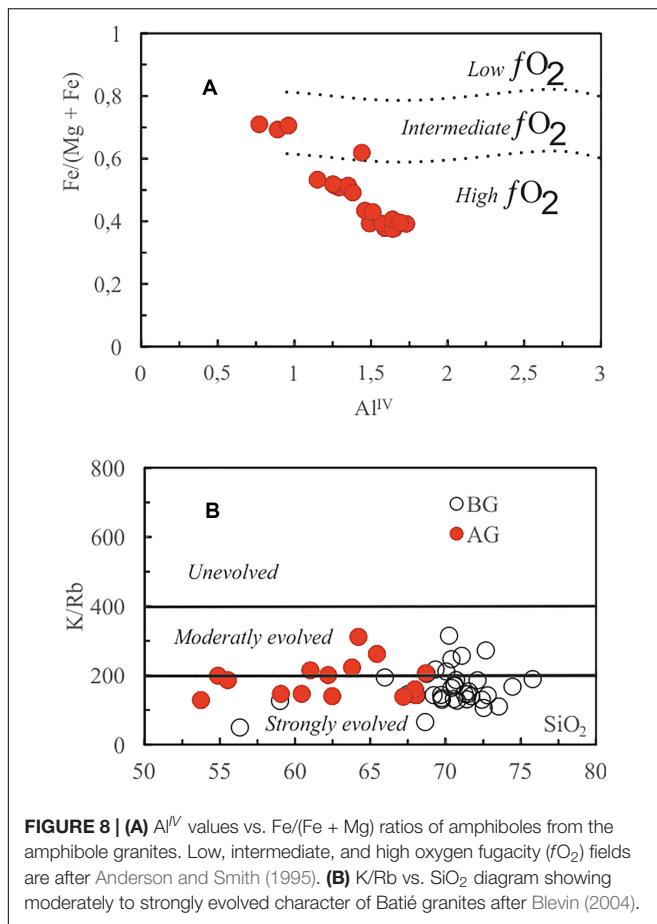
Petrogenesis

High-temperature granites are more prospective for mineralization because they have a greater capacity to undergo extended fractional crystallization and concentrate incompatible



components, including progressive increase in the activity of H_2O (Chappell et al., 1998). Barium variation in Batié granite illustrates that the compositional variation resulted from fractional crystallization. The Ba contents in the AG increased up to 2,000 ppm before decreasing. In the BG, Ba decreases

progressively and indicates biotite and K-feldspar crystallization. Negative Eu, Nb, Ta, P, and Ti anomalies indicate crystallization of minerals, such as plagioclase, hornblende, biotite, apatite, allanite, and titanite, in the magma of the Batié granites. The general decrease of certain elements, such as Fe_2O_3 , MgO, CaO,



TiO_2 , and Al_2O_3 , with increasing SiO_2 of the rocks can also be interpreted as evidence of fractional crystallization and/or magma mixing. However, the SiO_2 contents in both granites (AG and BG) exhibit linear correlations with P_2O_5 and Zr (Lee and Bachmann, 2014), indicating that magma mixing occurred rather than fractional crystallization. Mineralogical and geochemical compositions of Batié granites are similar to those of K-rich and K-feldspar porphyritic Calc-alkaline Granitoids (KCG) of mixed origin (Barbarin, 1999). However, the correlation between the initial ratios of Sr in the $^{87}Sr/^{86}Sr$ vs. SiO_2 or $1/Sr \cdot 10^3$ diagrams (Figures 9A,B) suggests a more complex process. Some samples of the biotite granite are arranged on a horizontal line, indicating fractional crystallization. On the other hand, the majority of samples have a negative correlation in both diagrams. According to Benito et al. (1999), this negative correlation is related to metasomatism caused by fluids from sediments.

High-temperature I-type granites are usually formed by the partial melting of mafic rocks in the deep crust or perhaps from a subduction modified mantle (Chappell et al., 1998). The diagram $Al_2O_3 + Fe_2O_3 + MgO + TiO_2$ vs. $Al_2O_3/(Fe_2O_3 + MgO + TiO_2)$ from Patiño Douce (1999) indicates that the amphibole granite melt was from amphibolite melts, whereas the biotite granite melt was from greywacke melts (Figure 9C). These melts are formed in the lower lithospheric crust. The isotopic data are not sufficient enough

to decide the origin of the magma of these granites. The initial Sr ratios (0.7019–0.7080; Supplementary Table S2) suggest a modified mantle source, whereas the ϵNdt values (–12.6 to –8.9) support a crustal source, although the value (–8.9) of the AG sample alone would indicate the possible mixing of amphibolite magmas and crustal felsic source. Moreover, the initial ratio $^{87}Sr/^{86}Sr = 0.7062 \pm 0.0012$ obtained by the isochron is that of the continental crust (Figure 3D). The Nd model ages (1,815–1,963 Ma for BG and 1,685 Ma for AG; Supplementary Table S2) probably suggest the age of the protolith rock source or mixing between juvenile mantle-derived material and melt from old (Eburnian) crust. Indeed, alkali-calcic granites are considered to be derived from hybrid sources, which are granites of crustal + mantle origin (Pupin, 1980; Barbarin, 1999). Furthermore, two samples of the amphibole granite are plotted around the lower continental crust, whereas the other samples (BG and AG) are around the upper continental crust in the Th/Nb vs. La/Nb diagram (Figure 9D). According to Barbarin (1999), KCG is derived from the mixing of mantle-derived basaltic magmas and crustal melts with varying proportions. Th/Nb ratios suggest the interaction between low continental crust (LCC) and upper continental crust (UCC) (Figure 9D). The crustal component is very important in the Batié granite than the other calc-alkaline granites of the West Cameroon region that are formed by magmatic mixing processes. The geological environment of the region also supports this hypothesis. In the Batié area, the continental basement is represented by Eburnian garnet gneiss (ca. 2.1 Ga) and Archaean rocks of the Congo craton. It is possible that one of these rocks participated in the formation of the magma of the Batié granite. Furthermore, recent work by Fozing et al. (2019) mentions amphibolite enclaves (with $Nd T_{DM} = 1.7$ Ga; see Kwékam et al., 2010) along the Kekem–Fotouni shear zone in the Fomopéa complex. These amphibolites may be representative of the type of basaltic magma from the lower crust that mixed with felsic magma derived from the upper crust. The most likely source for the granites of the Batié massif would be a crustal source resulting from the partial melting of heterogeneous materials from the deep basal layer (amphibolite) of the crust and the upper continental crust.

Geodynamic Context

The strongly potassic alkali-calcic characteristic with a shoshonite affinity and its high-temperature I-type granite feature show that the rocks of the Batié massif are derived from magma formed in an environment related to a subduction zone. Previous work along the TBF (Nguessi-Tchankam et al., 1997; Njonfang et al., 2006; Kwékam et al., 2010, 2013; Fozing et al., 2019) suggested an old plate boundary subducted during the assembling of blocks to form Gondwana. Liégeois et al. (2013) also indicate that this Pan-African structure represents the northern edge of the Congo craton (Figure 1). However, the ages obtained on the Batié granites make it possible to propose their emplacement during the Pan-African orogeny, which is more precisely at the end of crustal thickening (ca. 630–620 Ma) and continued to the left lateral wrench movements (610–580 Ma) (Ngako et al., 2008). This hypothesis is supported by the position of the samples of the two granites (AG and BG) in the geotectonic

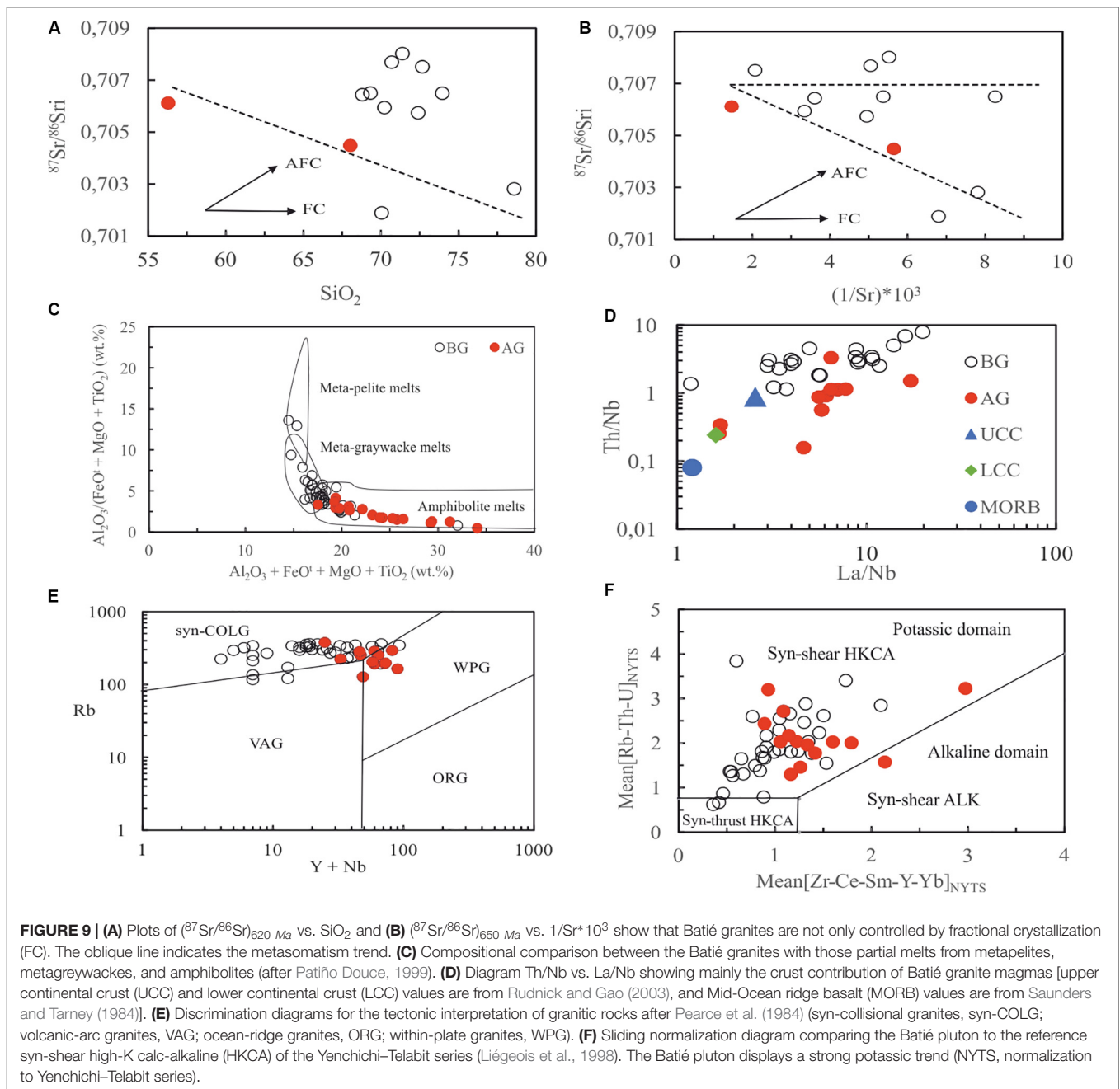


diagram Rb vs. $(Y + \text{Nb})$ of **Figure 9E**, where they mainly occupy the domains of syn-collisional granites (syn-COLG) and post-collisional granites by Pearce et al. (1984). Similarly in the diagram by Liégeois et al. (1998), the Batié rocks follow the potassic trend in the syn-shear high-K calc-alkaline (HKCA) domain (**Figure 9F**). At the end of its emplacement, the Batié massif was affected by right lateral wrench movements (ca. 585–540 Ma) marked at the northwestern edge by a NE–SW mylonite band (see **Supplementary Table S1** and **Figures 1, 2**). The right lateral wrench movements are mainly marked by the CCSZ (Ngako et al., 2008). The model for the emplacement of the Batié massif is very close to that

proposed by Ferré et al. (1998) for the granites of eastern Nigeria and Kwékam et al. (2010) for the Fomopéa pluton. The geodynamic context of the magma emplacement, starting with convergence and high-heat production, can last longer than in frontal collision orogeny and continue by strike-slip shear zones, which provide an ascent path. The origin of the Batié massif could be associated with the Pan-African convergence between the Congo craton and the Saharan metacraton that initiated the metacratonization of the northern boundary of the Congo craton. Post-collisional transpressive movements (Ngako et al., 2003; Tagne-Kamga, 2003; Kwékam et al., 2013) along the CCSZ induce linear lithospheric delamination, followed

by the upwelling of mantle magmas, triggering the partial melting of the old lower continental crust of the Congo craton's northern boundary. However, high-K alkali-calcic metaluminous granites are associated with delamination of over thickened crust (Frost et al., 2001).

CONCLUSION

The Pan-African post-collisional Batié granite at the southern edge of the Kekem–Fotouni shear zone (TBF fragment) in West Cameroon comprises biotite granite and amphibole granite, which is emplaced between 630 and 547 Ma during the transitional period between the crustal thickening (ca. 630–610 Ma) and the development of the shear zones first (610–580 Ma) sinistral and then dextral movements (585–540 Ma) and exhumed in a transpressive dextral NE–SW strike-slip tectonic setting. The presence of titanite, allanite, and magnetite associated with quartz shows that these highly potassic alkali-calcic granites are derived by partial melting of lower amphibolite deep crust and crystallized in a highly oxidizing H₂O-rich environment. Indeed, the granites of Batié were formed from highly evolved magma for the biotite granite to moderately evolved magma for the amphibole granite. These are high-temperature granites susceptible to mineralization. The mainly low initial (⁸⁷Sr/⁸⁶Sr)_{620 Ma} ratios (0.7062–0.7080) in combination with εNd_{620 Ma} (-12.6 to -8.9) suggest an abundant proportion of crustal material, supporting the participation of the old Paleoproterozoic crust in the formation of the Batié granite magma as indicated by their Nd T_{DM} ages (1.68–1.96 Ga). The results of this work indicate that there were successive phases of movement along the CCSZ, and that at each phase, it is associated with one granite series.

DATA AVAILABILITY STATEMENT

All datasets presented in this study are included in the article/**Supplementary Material**.

AUTHOR CONTRIBUTIONS

MK: conceptualization (lead), data curation (equal), formal analysis (equal), funding acquisition (equal), methodology

REFERENCES

- Abdel-Rahman, A. F. M. (1994). Nature of biotites from alkaline, calc-alkaline, and peraluminous magmas. *J. Petrol.* 35, 525–541. doi: 10.1093/petrology/35.2.525
- Abdelsalam, M. G., Liégeois, J. P., and Stern, R. J. (2002). The saharan metacraton. *J. Earth Sci.* 34, 119–136. doi: 10.1016/S0899-5362(02)00013-1
- Anderson, J. L., and Smith, D. R. (1995). The effects of temperature and (O₂ on the Al-in-hornblende barometer. *Am. Mineral.* 80, 549–559. doi: 10.2138/am-1995-5-614
- Barbarin, B. (1999). A review of the relationships between granitoid types, their origins and their geodynamic environments. *Lithos* 46, 605–626. doi: 10.1016/S0024-4937(98)00085-1

(equal), validation (lead), visualization (lead), writing – original draft (lead), and writing – review and editing (lead). VT: formal analysis (equal), investigation (equal), and writing. EF: data curation (equal), formal analysis (equal), investigation (equal), and writing – review and editing (equal). JT: data curation (equal), investigation (equal), software (equal), and writing – review (equal). ID: data curation (equal), formal analysis (equal), methodology (equal), software (equal), validation (equal), and writing – review and editing (equal). EN: conceptualization (equal), formal analysis (supporting), project administration (supporting), and writing – review. All authors contributed to the article and approved the submitted version.

ACKNOWLEDGMENTS

We thank the Germany Academic Exchange Organisation (DAAD) for its financial support. MK thanks Gerhard Wörner of the Universität Göttingen for his supervision and his team, especially Andreas Kronz for his help on electron microprobe and Gerald Hartman for additional isotope analyses. We are grateful to the anonymous reviewers whose pertinent remarks contributed to improving the quality of the manuscript. We are grateful to GS (co-editor of this special issue), Ana Rodrigues (Frontiers fee support), and Ursuala Rabar (Frontiers liaison manager) for their assistance in obtaining funding for publishing fees.

SUPPLEMENTARY MATERIAL

The Supplementary Material for this article can be found online at: <https://www.frontiersin.org/articles/10.3389/feart.2020.00363/full#supplementary-material>

TABLE S1 | Laser ablation ICP-MS U-Pb data on zircon from Amphibole granite, sample BT901.

TABLE S2 | Rb-Srand Sm-Ndwhole-rock data (Model age calculated after Michard et al. (1985).

TABLE S3 | Major and trace elements analyses.

TABLE S4 | Selected microprobe analyses of amphibole from amphibole granite.

TABLE S5 | Selected microprobe analyses of biotite.

- Barbey, P., Macaudière, J., and Nzenti, J. P. (1990). High-pressure dehydration melting of metapelites: evidence from the migmatites of Yaoundé (Cameroon). *J. Petrol.* 31, 401–427. doi: 10.1093/petrology/31.2.401
- Benito, R., Lopez-Ruiz, J., Cebria, J. M., Hertogen, J., Doblás, M., Oyarzun, R., et al. (1999). Sr and O isotope constraints on source and crustal contamination in the high-K calc-alkaline and shoshonitic neogene volcanic rocks of SE Spain. *Lithos* 46, 773–802. doi: 10.1016/S0024-4937(99)00003-1
- Blevin, P. L. (2004). Redox and compositional parameters for interpreting the granitoid metallogeny of Eastern Austria: implications for gold-rich ore system. *Resour. Geol.* 54, 241–252. doi: 10.1111/j.1751-3928.2004.tb00205.x
- Blundy, J. D., and Holland, T. J. B. (1990). Calcic amphibole equilibrium and a new amphibole-plagioclase geothermometer. *Contribut. Mineral. Petrol.* 104, 208–224. doi: 10.1007/BF00306444

- Bonin, B. (1990). From orogenic to anorogenic setting: evolution of granitic suites after a major orogenesis. *Geol. J.* 25, 261–270. doi: 10.1002/gj.3350250309
- Bosch, D., Bruguier, O., and Pidgeon, R. T. (1996). The evolution of an Archaean metamorphic belt: a conventional and SHRIMP U-Pb study of accessory minerals from the Jimpending metamorphic belt, Yilgarn craton, Western Australia. *J. Geol.* 104, 695–711. doi: 10.1086/629863
- Bouyo-Houketchang, M., Penaye, J., Njel, U. O., Moussango, A. P. I., Sep, J. P. N., Nyama, B. A., et al. (2016). Geochronological, geochemical and mineralogical constraints of emplacement depth of TTG suite from the Sinassi batholith in the central African Fold Belt (CAFB) of northern Cameroon: Implications for tectonomagmatic evolution. *J. African Earth Sci.* 116, 9–41. doi: 10.1016/j.jafrearsci.2015.12.005
- Castaing, C., Feybesse, J. L., Thieblemont, D., Triboulet, C., and Chevremont, P. (1994). Palaeogeographical reconstructions of the Pan-African/Brasiliano Orogen; closure of an oceanic domain or intracontinental convergence between major blocks? *Precamb. Res.* 69, 327–344. doi: 10.1016/0301-9268(94)90095-7
- Chappell, B. W., Bryant, C. J., Wyborn, D., White, A. J. R., and Williams, I. S. (1998). High- and Low-temperature I-type granites. *Ressour. Geol.* 48, 225–235. doi: 10.1111/j.1751-3928.1998.tb00020.x
- Chappell, B. W., and White, A. J. R. (1992). I- and S-type granites in the Lachlan Fold Belt. *Trans. R. Soc. Edinburg. Earth Sci.* 83, 1–26. doi: 10.1017/S0263593300007720
- Chen, M., Sun, M., Buslov, M. M., Cai, K., Zhao, G., Kulikova, V. A., et al. (2016). Crustal melting and magma mixing in a continental arc setting: evidence from the Yaloman intrusive complex in the Gorny Altai terrane, Central Asian Orogenic Belt. *Lithos* 252–253, 76–91. doi: 10.1016/j.lithos.2016.02.016
- Clowe, C. A., Popp, R. K., and Fritz, S. J. (1988). Experimental investigation of the effect of oxygen fugacity on ferric-ferrous ratios and unit-cell parameters of four natural clinopyroxenes. *Am. Mineral.* 73, 487–499.
- Dawaï, D., Bouchez, J. L., Paquette, J. L., and Tchameni, R. (2013). The Pan-African quartz-syenite of Guider (North-Cameroon): magnetic fabric and U-Pb dating of a late-orogenic emplacement. *Precamb. Res.* 236, 132–144. doi: 10.1016/j.precambres.2013.07.008
- Djouka-Fonkwé, M. L., Schulz, B., Schüssler, U., Tchouankoué, J.-P., and Nzolang, C. (2008). Geochemistry of the Bafoussam Pan-African I- and S-type granitoids in western Cameroon. *J. African Earth Sci.* 50, 148–167. doi: 10.1016/j.jafrearsci.2007.09.015
- Dumort, J.-C. (1968). Carte Géologique de Reconnaissance à l'échelle du 1/50000, République Fédérale du Cameroun, Notice Explicative Sur la Feuille Douala-Ouest, Direction des Mines et de la Géologie du Cameroun.
- Dunkl, I., Mikes, T., Simon, K., and von Eynatten, H. (2008). "Brief introduction to the windows program Pepita: data visualization, and reduction, outlier rejection, calculation of trace element ratios and concentrations from LA-ICP-MS data," in *Laser Ablation ICP-MS in the Earth Sciences: Current Practices and Outstanding Issues*. Mineralogical Association of Canada, Short Course, ed. P. Sylvester (Quebec City, QC: Mineralogical Association of Canada), 334–340.
- Ferré, E., Cabyl, R., Peucat, J. J., Capdevila, R., and Monié, P. (1998). Pan-African, post-collisional, ferro-potassic granite and quartz-monzonite plutons of Eastern Nigeria. *Lithos* 45, 255–279. doi: 10.1016/S0024-4937(98)00035-8
- Foster, M. (1960). Interpretation of the composition of trioctahedral micas. *U.S. Geol. Surv. Prof. Pap.* 354, 11–49. doi: 10.3133/pp354B
- Fozing, E. M., Kwékam, M., Gountié Dedzo, M., Asaah Asobo, N. E., Njanko, T., Tcheumenak Kouémo, J., et al. (2019). Petrography and geochemistry of amphibolites from the Fomopéa Pluton (West Cameroon): origin and geodynamic setting. *J. African Earth Sci.* 154, 181–194. doi: 10.1016/j.jafrearsci.2019.03.024
- Fozing, E. M., Kwékam, M., Njanko, T., Njonfang, E., Séta, N., Yakeu Sandjo, A. F., et al. (2014). Structural evolution of the Pan-African Misajé pluton (Northwestern Cameroon). *Syllab. Rev. Sci. Ser.* 5, 12–26.
- Frost, B. R., Barnes, C. G., Collins, W. J., Arculus, R. J., Ellis, D. J., and Frost, C. D. (2001). A geochemical classification for granitic rocks. *J. Petrol.* 42, 2033–2048. doi: 10.1093/ptrology/42.11.2033
- Hollister, L. S., Grissom, G. C., Peters, E. K., Stowell, H. H., and Sisson, S. B. (1987). Confirmation of the empirical correlation of Al in hornblende with pressure of solidification of calc-alkaline plutons. *Am. Mineral.* 72, 231–239.
- Jackson, S., Pearson, N., Griffin, W., and Belousova, E. (2004). The application of laser ablation-inductively coupled plasma-mass spectrometry to situ U-Pb zircon geochronology. *Chem. Geol.* 211, 47–69. doi: 10.1016/j.chemgeo.2004.06.017
- Johnson, M. C., and Rutherford, M. J. (1989). Experimental calibration of the aluminium-in-hornblende geobarometer with application to Long valley caldera (California) volcanic rocks. *Geology* 17, 841–867. doi: 10.1130/0091-7613(1989)017<0837:ECOTAI>2.3.CO;2
- Kwékam, M., Affaton, P., Bruguier, O., Liégeois, J.-P., Hartmann, G., and Njonfang, E. (2013). The Pan-African Kekem gabbro-norite (West-Cameroon), U-Pb zircon age, geochemistry and Sr-Nd isotopes: geodynamical implication for the evolution of the Central African fold belt. *J. African Earth Sci.* 84, 70–88. doi: 10.1016/j.jafrearsci.2013.03.010
- Kwékam, M., Dunkl, I., Fozing, E. M., Hartmann, G., Njanko, T., Tcheumenak Kouémo, J., et al. (2020). Syn-kinematic ferroan high-K I-type granites from Dschang in South-western Cameroon: U-Pb age, geochemistry and implications for crustal growth in the late Pan-African orogeny. *Geol. Soc.* 502:19. doi: 10.1144/sp502-2019-19
- Kwékam, M., Liégeois, J.-P., Njonfang, E., Affaton, P., Hartmann, G., and Tchoua, F. (2010). Nature, origin, and significance of the Fomopéa Pan-African high-K calc-alkaline plutonic complex in the Central African fold belt (Cameroon). *J. African Earth Sci.* 54, 79–95. doi: 10.1016/j.jafrearsci.2009.07.012
- Leake, B. E., Woolley, A. R., Arps, C. E. S., Birch, W. D., Grice, M. C., Hawthorne, F. C., et al. (1997). Nomenclature of amphiboles: report of the subcommittee on amphiboles of the international mineralogical association, commission on new minerals and mineral names. *Can. Mineral.* 35, 219–246.
- Lee, C.-T. A., and Bachmann, O. (2014). How important is the role of crystal fractionation in making intermediate magmas? Insights from Zr and P systematics. *Earth Planet. Sci. Lett.* 393, 266–274. doi: 10.1016/j.epsl.2014.02.044
- Li, X. H., Chen, Y., Tchouankoué, J. P., Liu, C. Z., and Li, J. (2017). Improving geochronological framework of the Pan-African orogeny in Cameroon: new SIMS zircon and monazite U-Pb age constraints. *Precamb. Res.* 294, 307–321. doi: 10.1016/j.precambres.2017.04.006
- Liégeois, J. P., Abdelsalam, M. G., Ennih, N., and Ouabadi, A. (2013). Metacraton: nature, genesis and behavior. *Gondw. Res.* 23, 220–237. doi: 10.1016/j.gr.2012.02.016
- Liégeois, J.-P., Navez, J., Hertogen, J., and Black, R. (1998). Contrasting origin of post-collisional high-K calc-alkaline and shoshonitic versus alkaline and peralkaline granitoids. The use of sliding normalization. *Lithos* 45, 1–28. doi: 10.1016/S0024-4937(98)00023-1
- Ludwig, K. R. (2012). User's Manual for Isoplot 3.75: A Geochronological Toolkit for Microsoft Excel. Berkeley Geochronology Center Special Publication, no. 4, p. 70. Available online at: http://www.bgc.org/isoplot_etc/isoplot/Isoplot3_75_4_15manual.pdf
- Maniari, P. D., and Piccoli, P. M. (1989). Tectonic discrimination of granitoids. *Geol. Soc. Am. Bull.* 101, 635–643. doi: 10.1130/0016-7606(1989)101<0635:TDOG>2.3.CO;2
- Marre, J. (1982). Méthodes d'analyse structurale des granitoïdes. *B.R.G.M. Manuels et Méthodes* 3:128.
- McDonough, W. F., Sun, S.-S., Ringwood, A. E., Jagoutz, E. A. W., and Hofmann, A. W. (1992). Potassium, rubidium, and cesium in the Earth and Moon and the evolution of the mantle of the Earth. *Geochim. Cosmochim. Acta* 56, 1001–1012. doi: 10.1016/0016-7037(92)90043-I
- Michard, A., Gurriet, P., Soudan, M., and Albarède, F. (1985). Nd isotopes in French Phanerozoic shales: external vs internal aspects of crustal evolution. *Geochim. Cosmochim. Acta* 49, 601–610. doi: 10.1016/0016-7037(85)90051-1
- Ngako, V., Affaton, P., and Njonfang, E. (2008). Pan-African tectonic in northwestern Cameroon: implication for history of Western Gondwana. *Gondw. Res.* 14, 509–522. doi: 10.1016/j.gr.2008.02.002
- Ngako, V., Affaton, P., Nnange, J. M., and Njanko, T. (2003). Pan-African tectonic evolution in central and southern Cameroon: transpression and transtension during sinistral shear movements. *J. African Earth Sci.* 36, 207–214. doi: 10.1016/S0899-5362(03)00023-X
- Nguiessi-Tchankam, Cl, Nzenti, J. P., Nsifa, E. N., Tempier, P., and Tchoua, F. (1997). A calc-alkaline magmatic complex from Bandja in the north-equatorial fold belt; a synkinematic emplacement of plutonic rocks in a sinistral strike-slip shear zone from Pan-African age. *Compt. Rend. Acad. Sci. Paris* 325, 95–101. doi: 10.1016/S1251-8050(97)83969-9

- Njanko, T., Njiki Chatué, C., Kwékam, M., Bella Nké, B. E., Yakeu Sandjo, A. F., and Fozing, E. M. (2017). The Numba ductile deformation zone (northwest Cameroon): a geometric analysis of folds based on the Fold Profiler method. *J. Earth Syst. Sci.* 126, 23–33. doi: 10.1007/s12040-017-0801-7
- Njiekak, G., Dörr, W., Tchouankoué, J.-P., and Zulauf, G. (2008). U-Pb zircon and microfabric data of (meta) granitoids of western Cameroon: constraints on the timing of pluton emplacement and deformation in the Pan-African belt of central Africa. *Lithos* 102, 460–477. doi: 10.1016/j.lithos.2007.07.020
- Njonfang, E., Ngako, V., Kwékam, M., and Affaton, P. (2006). Les orthogneiss calco-alcalins de Foumban-Bankim: témoins d'une zone interne de marge active panafricaine en cisaillement. *Compt. Rend. Geosci.* 338, 606–616. doi: 10.1016/j.crte.2006.03.016
- Nzenti, J. P., Ngako, V., Kambou, R., Penaye, J., Bassahak, J., and Njel, U. O. (1992). Structures regionales de la chaîne panafricaine au Nord-Cameroun. *Compt. Rend. Acad. Sci. Paris* 611, 115–119.
- Nzolang, C., Kagami, H., Nzenti, J. P., and Holtz, F. (2003). Geochemistry and preliminary Sr-Nd isotopic data on the neoproterozoic granitoids from the Bantoum area, west Cameroon: evidence for a derivation from a Paleoproterozoic to Archean crust. *Pol. Geosci.* 16, 196–226.
- Patiño Douce, A. E. (1999). What do experiments tell us about the relative contributions of crust and mantle to the origin of granitic magmas? *Geol. Soc. Lond. Spec. Public.* 168, 55–75. doi: 10.1144/GSL.SP.1999.168.01.05
- Pearce, J. A., Harris, N. B. W., and Tindle, A. G. (1984). Trace element discrimination diagrams for the tectonic interpretation of granitic rocks. *J. Petrol.* 25, 956–983. doi: 10.1093/petrology/25.4.956
- Peccerillo, A., and Taylor, S. R. (1976). Geochemistry of eocene calc-alkaline volcanic rocks from the Kastamonu area, Northern Turkey. *Contribut. Mineral. Petrol.* 58, 63–81. doi: 10.1007/BF00384745
- Penaye, J., Toteu, S. F., Van Schumus, W. R., and Nzenti, J. P. (1993). U-Pb and Sm-Nd Preliminary geologic data on the Yaoundé séries Cameroon. Reinterpretation of the granulitic rocks as suture of a collision in the "Central African" belt. *Compt. Rend. Acad. Sci. Paris* 317, 789–794.
- Pouchou, J. L., and Pichoir, F. (1984). A new model for quantitative X-ray microanalysis of homogeneous samples. *Rech. Aérop.* 5, 13–38.
- Pupin, J. P. (1980). Zircon and granite petrology. *Contribut. Mineral. Petrol.* 73, 207–220. doi: 10.1007/BF00381441
- Rickwood, P. C. (1989). Boundary lines within petrologic diagrams which use oxides of major and minor elements. *Lithos* 22, 247–263. doi: 10.1016/0024-4937(89)90028-5
- Ridolfi, F., Renzulli, A., and Puerini, M. (2010). Stability and chemical equilibrium of amphibole in calc-alkaline magmas: an overview, new thermobarometric formulations and application to subduction-related volcanoes. *Contribut. Mineral. Petrol.* 160, 45–66. doi: 10.1007/s00410-009-0465-7
- Rudnick, R. L., and Gao, S. (2003). "Composition of the continental crust" in *The Crust, Treatise in Geochemistry*, Vol. 3, eds R. L. Rudnick, H. D. Holland, and K. K. Turekian (Amsterdam: Elsevier), 1–16. doi: 10.1016/B0-08-043751-6/03016-4
- Saunders, A. D., and Tarney, J. (1984). "Geochemical characteristic of basaltic volcanism within back-arc basins," in *Marginal Basin Geology*, eds B. P. Kokelaar and M. F. Howells (London: Geology Society), 59–76. doi: 10.1144/GSL.SP.1984.016.01.05
- Schmidt, M. (1992). Amphibole composition in tonalite as a function of pressure: an experimental calibration of the Al-in-hornblende barometer. *Contribut. Mineral. Petrol.* 110, 304–310. doi: 10.1007/BF00310745
- Sláma, J., Košler, J., Condon, D. J., Crowley, J. L., Gerdes, A., Hanchar, J. M., et al. (2008). Plešovice zircon - A new natural reference material for U-Pb and Hf isotopic microanalysis. *Chem. Geol.* 249, 1–35. doi: 10.1016/j.chemgeo.2007.11.005
- Sun, S. S. (1982). Chemical composition and origin of the earth's primitive mantle. *Geochim. Cosmochim. Acta* 46, 179–192. doi: 10.1016/0016-7037(82)90245-9
- Tagne-Kamga, G. (2003). Petrogenesis of the neoproterozoic ngondo plutonic complex (Cameroon, west central Africa): a case of late-collisional ferro-potassic magmatism. *J. African Earth Sci.* 36, 149–171. doi: 10.1016/S0899-5362(03)00043-5
- Talla, V. (1995). *Le Massif Granitique Panafricain de Batié (Ouest Cameroun): Pétrologie-Péetrostructurale-Géochimie*. Thèse Doctorat 3ème cycle, Université de Yaoundé I, Yaoundé.
- Tchameni, R., Pouclet, A., Penaye, J., Ganwa, A. A., and Toteu, S. F. (2006). Petrology and geochemistry of the Ngaoundéré Pan-African granitoids in central north Cameroon: implications for their sources and geological setting. *J. African Earth Sci.* 44, 511–529. doi: 10.1016/j.jafrearsci.2005.11.017
- Tcheumenak Kouémo, J., Njanko, T., Kwékam, M., Naba, S., Bella Nké, B. E., Yankeu Sandjo, A. F., et al. (2014). Kinematic evolution of the Fodjomekwet-Fotouni Shear Zone (West-Cameroon): implication on the emplacement of the Fomopéa and Bandja plutonic massifs. *J. African Earth Sci.* 99, 261–275. doi: 10.1016/j.jafrearsci.2014.07.018
- Tchouankoué, J. P., Li, X. H., Ngo Belnoun, R. N., Mouafo, L., and Ferreira, V. P. (2016). Tinning and tectonic implications of the Pan-African Bangangté syenomonzonite: constraints from in-situ zircon U-Pb age and Hf-O isotopes. *J. African Earth Sci.* 124, 94–103. doi: 10.1016/j.jafrearsci.2016.09.009
- Tetsopgang, S., Suzuki, K., and Njonfang, E. (2008). Petrology and CHIME geochronology of Pan-African high-K and Sr/Y granitoids in the Nkambé area, Cameroon. *Gondw. Res.* 14, 686–699. doi: 10.1016/j.gr.2008.01.012
- Toteu, S. F., Fouateu, Y. R., Penaye, J., Tchakounté, J., Mouangue, S. C. A., Van Schmus, R. W., et al. (2006). U-Pb dating of plutonic rocks involved in the nape tectonic in Southern Cameroon: consequence for the Pan-African orogenic evolution of the central African fold belt. *J. African Earth Sci.* 44, 479–493. doi: 10.1016/j.jafrearsci.2005.11.015
- Toteu, S. F., Penaye, J., and Poudjoun-Djomani, Y. H. (2004). Geodynamic evolution of the Pan-African belt in Central Africa with special reference to Cameroon. *Can. J. Earth Sci.* 41, 73–85. doi: 10.1139/e03-079
- Toteu, S. F., Van Schmus, W. R., Penaye, J., and Michard, A. (2001). New U-Pb and Sm-Nd data from north-central Cameroon and its bearing on the pre-Pan African history of central Africa. *Precamb. Res.* 108, 45–73. doi: 10.1016/S0301-9268(00)00149-2
- Wiedenbeck, M., Allé, P., Corfu, F., Griffin, W. L., Meier, M., Oberli, F., et al. (1995). Three natural zircon standards for U-Th-Pb, Lu-Hf, trace element and REE analyses. *Geostand. Newslett.* 19, 1–23. doi: 10.1111/j.1751-908X.1995.tb00147.x
- Wones, D. R. (1981). Mafic silicates as indicators of intensive variables in granitic magmas. *Min. Geol.* 31, 191–212.
- Wones, D. R. (1989). Significance of the assemblage titanite + magnetite + quartz in granitic rocks. *Am. Mineral.* 74, 744–749.

Conflict of Interest: The authors declare that the research was conducted in the absence of any commercial or financial relationships that could be construed as a potential conflict of interest.

Copyright © 2020 Kwékam, Talla, Fozing, Tcheumenak Kouémo, Dunkl and Njonfang. This is an open-access article distributed under the terms of the Creative Commons Attribution License (CC BY). The use, distribution or reproduction in other forums is permitted, provided the original author(s) and the copyright owner(s) are credited and that the original publication in this journal is cited, in accordance with accepted academic practice. No use, distribution or reproduction is permitted which does not comply with these terms.